Similar controls on calcification under ocean acidification across unrelated coral reef taxa

Steeve Comeau, Christopher E Cornwall, Thomas M Decarlo, Erik Krieger, Malcolm Mcculloch

Primary Research Article

Similar controls on calcification under ocean acidification across unrelated coral reef taxa

Running head: Calcification physiology in coral reef taxa

Comeau S.[1,2,3,†*], Cornwall C.E. [1,2,4,†], De Carlo, T. M.[1,2], Krieger E. [1,4,5], McCulloch M. T.[1,2]

[1]The University of Western Australia, Oceans Graduate School, 35 Stirling Highway, Crawley 6009, Western Australia, Australia

[2]ARC Centre of Excellence for Coral Reef Studies, 35 Stirling Highway, Crawley 6009, Western Australia, Australia

[3]Sorbonne Université, CNRS-INSU, Laboratoire d'Océanographie de Villefranche, 181 chemin du Lazaret, F–06230 Villefranche-sur-mer, France

[4]Present address: School of Biological Sciences, Victoria University of Wellington, Wellington 6010, New Zealand

[5]University of Bremen, Fachbereich 2 Biologie/Chemie, Bremen, Germany

[†]SC and CEC contributed equally

[*]Corresponding author: steeve.comeau@obs-vlfr.fr, +33 4 93 76 38 01

Keywords: pH, Dissolved inorganic carbon, Calcifying fluid, Calcium, Physiology, Coral, Coralline alga

Abstract

Ocean acidification (OA) is a major threat to marine ecosystems, particularly coral reefs which are heavily reliant on calcareous species. OA decreases seawater pH and calcium carbonate saturation state (Ω), and increases the concentration of dissolved inorganic carbon (DIC). Intense scientific effort has attempted to determine the mechanisms via which ocean acidification (OA) influences calcification, led by early hypotheses that calcium carbonate saturation state (Ω) is the main driver. We grew corals and coralline algae for 8 to 21 weeks, under treatments where the seawater parameters Ω, pH and DIC were manipulated to examine their differential effects on calcification rates and calcifying fluid chemistry (Ω_{cf}, pH_{cf}, and DIC_{cf}). Here, using long duration experiments, we provide geochemical evidence that differing physiological controls on carbonate chemistry at the site of calcification, rather than seawater Ω, are the main determinants of calcification. We found that changes in seawater pH and DIC rather than Ω had the greatest effects on calcification and calcifying fluid chemistry, though the effects of seawater carbonate chemistry were limited. Our results demonstrate the capacity of organisms from taxa with vastly different calcification mechanisms to regulate their internal chemistry under extreme chemical conditions. These findings provide an explanation for the resilience of some species to OA, while also demonstrating how changes in seawater DIC and pH under OA influence calcification of key coral reef taxa.

Introduction

Over the last decade there has been intensive scientific effort to better understand the impacts of ocean acidification (OA) on calcifying organisms that are responsible for building and sustaining coral reefs. OA is expected to cause a reduction in calcification of both corals and coralline algae (Kroeker, Kordas, Crim, & Singh, 2010) that are key reef formers and cementing species in coral reefs (Chan & Connolly, 2013; McCoy & Kamenos, 2015). The reduction of calcification with OA has often been linked to the decrease in seawater Ω, because the precipitation of $CaCO_3$ ultimately requires both Ca^{2+} and CO_3^{2-}. Because $[Ca^{2+}]$ is constant in the oceans and will not be affected by OA, the decrease in calcification with OA has been attributed to the associated decrease in $[CO_3^{2-}]$. However, the capacity of organisms to transport seawater CO_3^{2-} across membranes has not been proven, which led to the alternate hypothesis that the ratio between seawater [DIC] and $[H^+]$ controls calcification (Bach et al., 2013; Jokiel, 2013). This hypothesis is based on the principle that skeletal accretion requires the import of DIC that is consumed, and export of H^+ that are produced during the mineralization process in the calcifying fluid (i.e., the site of calcification). Under this hypothesis, the decline in calcification under OA is caused by higher $[H^+]$ in seawater that increases the gradient against which H^+ need to be exported from the calcifying fluid (Jokiel, 2013; Jokiel, 2011). This steeper gradient could either reduce the capacity of the organisms to maintain elevated pH in the calcifying fluid (pH_{cf}), or increase the energy expenditure needed to maintain constant elevated pH_{cf} (McCulloch, Falter, Trotter, & Montagna, 2012; Venn et al., 2013). The role of DIC is more complex because the species of DIC involved (CO_3^{2-}, HCO_3^-, or CO_2), the mechanisms via which it is transported to the site of calcification in different taxa (Zoccola et al., 2015), and its origin (metabolic or inorganic) remain controversial (Furla, Galgani, Durand, & Allemand, 2000).

Attempts to disentangle the effects of these parameters of carbonate chemistry on calcification have collectively demonstrated that decreasing seawater DIC, pH, [DIC] / $[H^+]$ and Ω can all reduce calcification for various marine calcifiers (Comeau, Tambutté, et al., 2017; Comeau, Carpenter, & Edmunds, 2013; Herfort, Thake, & Taubner, 2008). However, results are inconsistent, indicating changes in $[CO_3^{2-}]$, $[HCO_3^-]$, Ω, [DIC] / $[H^+]$, and $[Ca^{2+}]$ could all influence calcification rates to varying

extents (Comeau, Tambutté, et al., 2017; Comeau et al., 2013; Herfort et al., 2008; Jury, Whitehead, & Szmant, 2010; Marubini, Ferrier-Pagès, Furla, & Allemand, 2008; Marubini, Ferrier-Pages, & Cuif, 2003; Schneider & Erez, 2006). The difficulty with testing these hypotheses is that [DIC] / $[H^+]$ and Ω are correlated, leading to an inability to test the role of one over the other (Comeau et al., 2013; Jokiel, 2011). Therefore, here we examine the underlying role of seawater carbonate chemistry parameters in the calcification process by testing the independent effects of [DIC], $[H^+]$, [DIC] / $[H^+]$ and Ω on calcification rates and calcifying fluid chemistry on multiple coral and coralline algal species. We choose to work on two different taxa (coral and coralline alga) to investigate if organisms with different physiologies and calcification mechanisms would respond similarly to large modification of the carbonate chemistry.

Past studies that have examined the separate effects of the different species of the carbonate system have had three limitations that we seek to overcome: 1) no test of the treatment conditions on multiple species representing a range of taxa, 2) short duration times (≤ 2 weeks, but mostly ~ 1 or 2 hours) where specimens are subject to "shock" responses, and most importantly 3) they have not determined the underlying processes responsible for the observed effects on calcification: specifically how pH, DIC, and Ω within the calcifying fluid where precipitation occurs is affected by the prescribed treatments.

To test these hypotheses, we grew the subtropical coral species *Pocillopora damicornis* and *Acropora yongei* for 13 and 8 weeks, and the coralline algal species *Neogoniolithon* sp. and *Sporolithon* for 21 weeks under 5 treatments (Figure 1 and Table S1) designed specifically to determine the effects: 1) of DIC at constant pH $[H^+]$, 2) of pH at constant [DIC], and 3) of changes in both [DIC] and pH at constant Ω. These treatments allowed us to isolate the effects of Ω from both [DIC] and $[H^+]$ on calcification rates and calcifying fluid chemistry. We purposely selected treatments that were not extreme, and within the ranges of past and realistic future seawater Ω expected over the next 100 years. The effects of these treatments on the chemistry at the site of calcification were assessed using newly developed suite of skeletal proxies of the carbonate chemistry of the calcifying fluid ($\delta^{11}B$, B/Ca, and FWHM measured by Raman spectroscopy).

Materials and Methods

Organism collection

The experiment was performed in two phases, the first in April–June 2016 and the second in August–October 2016. The first phase focused on the coral *P. damicornis* and the second phase on the coral *A. yongei*. The two CCA species were grown throughout both phases of the experiment, because their calcification rates are much slower than the coral, hence taking a longer period of time to grow the carbonate material needed for further geochemical analyses mentioned below. The experiment was carried out in the Indian Ocean Marine Research Centre at Watermans Bay, Western Australia, Australia. Organisms were collected 7 to 15 d prior to the beginning of the experiment from Salmon Bay, Rottnest Island, Western Australia, at ~ 1–2-m depth. After collection, the branches (~5 cm) were glued to plastic bases (4 x 4 cm) with Z-Spar (A788 epoxy) to facilitate handling of the nubbins without contact with the tissues.

Treatments and regulation of pH

Our experiment consisted of five treatments that were created in duplicate ~ 20 L black tanks for a total of 10 experimental tanks. Each experimental tank was attached to an individual header tank where seawater carbonate chemistry was manipulated as per Fig. 3a from Cornwall & Hurd (2016). Header tanks consisted of 220 L drums. The five treatments were specifically chosen to test the two hypotheses mentioned in the introduction. Combinations of CO_2-free air, pure CO_2, 2 M HCl, and 2 M NaOH were used to manipulate the seawater to the desired conditions. To avoid exposing organisms directly to large changes in seawater chemistry resulting from the addition of HCl and NaOH, seawater (pumped from 12-m depth 150-m off the shore) was first manipulated in the header tanks. Modified seawater was pumped into the experimental tanks every 3 hours for 15 min from each header tank to their respective incubation tanks to ensure the delivery of ~60 L of manipulated seawater per day, 3 times the experimental tank volume. Manipulations of the carbonate chemistry in the header tanks was done twice per week on new seawater by adjusting first the total alkalinity (A_T) using additions HCl or NaOH (Table S1). pH was then adjusted to the desired value using pH-controllers (AquaController, Neptune systems, USA) that controlled the bubbling of either pure CO_2 or CO_2-free air. During the 3 – 6 hours

necessary to equilibrate the seawater to the target pH, the delivery of seawater from the header tanks to the experimental tanks was suspended. pH was also continuously adjusted in each experimental tank using pH-controllers that controlled the bubbling of either CO_2-free air or pure CO_2.

Light was provided by 150W LED (Malibu LED, Ledzeal) that followed a natural diel cycle. Light was ramped up in the morning from 6:30 h until 10:30 h to a maximum of ~200 – 250 μmol quanta m^{-2} s^{-1} (for corals) or 30 – 40 μmol quanta m^{-2} s^{-1} (for CCA) that was maintained for 4 h before ramping down until total darkness at 18:30 h. Temperature was kept constant at ~20° C, which is the average annual seawater temperature in Salmon Bay (Ross, Falter, Schoepf, & McCulloch, 2015) where organisms were collected. Two submersible water pumps (Tunze) provided turbulent water motion in each incubation tank. This simulated more than 3 cm s^{-1} unidirectional seawater velocities. To avoid any nutritional stress, the corals were fed with freshly hatched brine shrimp twice per week.

Carbonate chemistry

Seawater pH and temperature were measured at 09:00 h every ~2 d in each incubation tank and after each water change in the drums, using a pH meter calibrated before each use on the total scale using Tris/HCl buffers, made following the protocol of (Dickson, Sabine, & Christian, 2007). A_T was measured twice per week in each incubation tank. A_T was calculated using a modified Gran function, as described in (Dickson, Sabine, Christian, 2007), and titrations of certified reference materials (CRM) provided by A.G. Dickson (batch 151) yielded A_T values within 3 μmol kg^{-1} of the certified value. A_T, pH_T, temperature, and salinity were used to calculate the carbonate chemistry parameters using the seacarb package running in R software (R Foundation for Statistical Computing).

Calcification rates

Prior to the incubation, the skeletons of the organisms were stained by placing the organisms during 18 hours in seawater enriched with the fluorescent dye calcein at 50 mg L^{-1} with a pH adjusted to ~8.1 by the addition of NaOH. Three individuals of each species were placed in random order within each of the 10 incubation tanks, and calcification was measured over the incubation periods using buoyant weighing. We acknowledge that housing organisms in the same tank is not ideal, but these

experimental treatments are logistically challenging to maintain for a long duration, and this level of replication equals or exceeds that used previously in these types of manipulations. Our experimental design also allows us to assess linear relationships between the different parameters of seawater carbonate chemistry and responses in multiple tanks, avoiding some of the pitfalls of traditional factorial approaches if they also implemented two tanks per treatment. The difference in buoyant weight between the beginning and end of incubation was converted to dry weight of aragonite and was used to calculate net calcification. Some *Neogonioltihon* sp. individuals died over the course of the experimental duration, so calcification rates at the 100 day mark where used for individuals that died between then and the end of the experiment. Mortality was similar across treatments. Calcification rates were normalized to surface area of the coral or CCA (mg cm^{-2} d^{-1}) determined using the aluminum foil method. The duration of the experiment was 21 weeks for the CCA, 13 weeks for *P. damicornis* and 8 weeks for *A. yongei*.

Net photosynthesis

Photosynthetic rates were determined on *A. yongei* after 6 weeks and on *S. durum* after 18 weeks in the experimental treatments. Each individual was placed into in a sealed incubation chamber filled with seawater originating from its respective tank. Light and temperature were adjusted to match the respective conditions in the tanks and a magnetic stirring bar was placed inside the incubation chambers to provide flow. Incubations lasted ~ 1.5 – 2h and dissolved oxygen (measured using an A323 dissolved oxygen portable meter, Orion Star, Thermo Scientific, USA) and temperature were recorded at the start and end of each incubation to calculate net photosynthesis. Controls with tank seawater were run during each incubation.

pH_{cf}, DIC_{cf}, and Ca_{cf}

Calcifying fluid pH (pH_{cf}) for all organisms and DIC (DIC_{cf}) for corals was calculated using the $\delta^{11}B$ proxy method for pH_{cf} (Trotter et al., 2011) and the $\delta^{11}B$ and B/Ca method for DIC_{cf} (Holcomb et al., 2016; McCulloch et al., 2017). Measurements of the skeleton geochemistry were done on the tip of the branches of corals (first 1–2 mm) that corresponded to material deposited during the incubation (as confirmed by the calcein staining). The selected portions of the skeleton were sampled by

sectioning apical tips and then were crushed in a mortar and pestle. Coralline algal sample preparation followed the methods of (Cornwall, Comeau, & McCulloch, 2017). Briefly, samples were placed for 24 hours in 6.25 % NaClO, rinsed in mQ water. Sections of corallines were then cut to determine the distance of the calcein stain from the surface of individual samples, and examined under a fluorescence compound microscope. To ensure that skeleton grown during the experimental trial was sampled, individuals were only further processed if the stain was more than 0.5 mm from the surface. Due to uneven calcification, this meant that some individuals did not have regions that could be sampled, while for other individuals only small areas could be sampled. A diamond studded rounded tip attached to a dental drill was used to remove surface material.

All powders were processed subsequently in the clean laboratory of the Advanced Geochemical Facility for Indian Ocean Research [AGFIOR, University of Western Australia (UWA)] for dissolution and dilution to 10-ppm Ca solutions. Ten mg of each sample was placed in 6.25 % NaClO for 15 mins, rinsed in MilQ water then dried for 24 h. Samples were then dissolved in 0.51 N HNO_3, and the boron was quantitatively separated on ion exchange columns and $\delta^{11}B$ was measured on a multicollector inductively coupled plasma mass spectrometry (NU II). Measurements of the international carbonate standard JCP-1 yielded a mean value of 24.47 ± 0.06 ‰ (mean ± SE, n = 7), which was similar to the 24.33 ± 0.11 ‰ (SE) reported previously. Calculations of pH_{cf} based on $\delta^{11}B$ were made using the calculations of (Trotter et al., 2011):

$$pH_{cf} = pK_B - \log\left[\frac{(\delta^{11}B_{SW} - \delta^{11}B_{carb})}{\left(\alpha_{(B3-B4)}\delta^{11}B_{carb} - \delta^{11}B_{SW} + 1000\,(\alpha_{(B3-B4)} - 1)\right)}\right] \quad (1)$$

where pK_B is the dissociation constant dependent on temperature and salinity, $\delta^{11}B_{sw}$ = 39.61 (Foster, Pogge von Strandmann, & Rae, 2010), and $\alpha_{B3\text{-}B4}$ is the boron isotopic fractionation factor for the pH dependent equilibrium of the borate ($B(OH)_4^-$) relative to the boric acid ($B(OH)_3$) species in the calcifying fluid, with a value of 1.0272 (Klochko, Kaufman, Yao, Byrne, & Tossell, 2006).

B/Ca ratios, measured on the same material, and $\delta^{11}B$ was utilized to determine [CO_3^{2-}] and then [DIC] at the site of calcification $[DIC]_{cf}$ following (McCulloch et al., 2017). B/Ca ratios were determined on the same aliquot of the solution used for pH_{cf} estimates and DIC_{cf} was calculated from estimates of carbonate

ion concentrations using the following equations described in (McCulloch et al., 2017):

$$[CO_3^{2-}]_{cf} = K_D[B(OH)_4^-]_{cf}/\left({}^{B}/_{Ca}\right)_{CaCO_3} \quad (2)$$

Where $K_D = K_{D.0}\exp(-k_{KD}[H^+]_T)$ with $K_{D,0} = 2.97 \pm 0.17\times10^{-3}$ (± 95% CI), $k_{K_D} = 0.0202 \pm 0.042$. The concentration of DIC_{cf} was then calculated from estimates of pH_{cf} and $[CO_3^{2-}]_{cf}$.

$[Ca^{2+}]_{cf}$ was calculated as:

$$[Ca^{2+}]_{cf} = {\Omega_{Ar} * K_{sp}}/{[CO_3^{2-}]_{cf}} \quad (1)$$

where $[CO_3^{2-}]_{cf}$ and Ω_{Ar} are derived from boron systematics and Raman spectroscopy (see below), respectively (DeCarlo et al., 2017). $Ca_{cf}^{2+}/Ca_{sw}^{2+}$ ratios were calculated by normalizing to $[Ca^{2+}]_{sw}$, which was estimated from salinity as 10.58 mmol kg^{-1}.

Raman spectroscopy

We utilized confocal Raman spectroscopy to determine sample mineralogy and as a proxy of calcifying fluid Ω. Measurements were conducted on a WITec Alpha300RA+ using a 785 nm infrared laser following (DeCarlo et al., 2017). The instrument is configured with a 1200 mm^{-1} grating that gives a spectral resolution of approximately 1.3 cm^{-1} and we used a 20x objective with 0.5 numerical aperture. Repeated analyses of a silicon chip for wavenumber calibration showed the primary Si peak located at ~522.9 cm^{-1}. Skeleton samples were placed on glass slides (powders for corals, and cut sections for CCA) and topography maps were made with the TrueSurface module. The automated stage followed the topography while conducting Raman measurements so that the optics were always in focus on the sample surfaces. For corals, 36 spectra were collected per sample in a 300 µm by 300 µm grid using 1 s integrations, whereas for CCA 100 spectra were collected in a 1 mm by 1 mm grid using 2 s integrations. Spectra with poor signal (< 100 intensity units) or contaminated by cosmic rays were excluded.

Sample mineralogy was determined by (1) the presence of a ν_1 peak at ~1085-1090 cm^{-1} indicative of $CaCO_3$, and (2) the shape of the ν_4 peak between 700-720 cm^{-1} where a double peak < 710 cm^{-1} is found in aragonite and a single peak > 710

cm^{-1} is found in calcite (Kamenos, Perna, Gambi, Micheli, & Kroeker, 2016; Urmos, Sharma, & Mackenzie, 1991). Identifying mineralogy is key for CCA because aragonite and/or gypsum has been found in their skeletons under naturally low-pH conditions (Kamenos et al., 2016) and mixtures of high-Mg calcite with these other mineral phases would complicate the interpretations of boron systematics. We found only aragonite in our coral samples and only high-Mg calcite in our CCA samples, confirming the mineralogy expected for each species (Figure S2).

The widths of the ν_1 peaks were used as proxy measures of calcifying fluid Ω (DeCarlo et al., 2017). $CaCO_3$ minerals precipitating from more supersaturated solutions incorporate more impurities and are more disordered, which causes Raman peak broadening due to greater distributions of C-O bond lengths (DeCarlo et al., 2017). We used the abiogenic aragonite calibration equation of (DeCarlo et al., 2017) to calculate Ω_a for the two coral species from the ν_1 full width at half maximum intensity (FWHM). Although ν_1 peak width has been applied to investigate CCA responses to ocean acidification in several studies (Kamenos et al., 2016; Kamenos et al., 2013), there is no abiogenic high-Mg calcite Ω calibration. We therefore used ν_1 FWHM as a qualitative proxy of CCA calcifying fluid Ω. However, the high concentrations of Mg in CCA are known to broaden the Raman peaks independent of Ω, meaning that standardization to [Mg] is required when comparing ν_1 FWHM among high-Mg calcite samples (DeCarlo et al., 2017), (Pauly, Kamenos, Donohue, & LeDrew, 2015). The abiogenic calibrations of (Perrin et al., 2016) were used to first estimate [Mg] from ν_1 wavenumber (following corrections based on comparing our Si chip wavenumber measurements to those reported by Perrin et al., 2016), and then to account for the effect of [Mg] on ν_1 FWHM. We consider the residual ν_1 FWHM a proxy measure of calcifying fluid Ω.

Statistical analysis

The assumptions of normality and equality of variance were evaluated through graphical analyses of residuals using the R software. Treatment effects were determined using one-way ANOVAs. The effect of seawater pH, DIC and saturation sates of aragonite or calcite (for corals and CCA respectively) on calcification, photosynthesis, pH_{cf}, DIC_{cf}, and Ω_a were examined using linear models when possible. Proportions of the variation (R^2) explained by pH, DIC and saturation sates of aragonite or calcite were calculated using multiple linear regressions and the R

304 package relaimpo. All statistical analysis were done with R.

305

306 **Results**

307 Our results show that only the calcification rates of *A. yongei* were affected by
308 our treatments (Table S2), where calcification decreased as seawater pH declined
309 (Figure 2, Table S3). In the three treatments where Ω was held constant, calcification
310 was similar in the Low DIC – High pH and the Ambient treatment and lower in the
311 High DIC – Low pH treatment. Calcification of *P. damicornis*, *S. durum* and
312 *Neogoniolithon* sp. was not significantly affected by any parameter of the seawater
313 chemistry over the ranges we tested (Figure 2, Table S2 and S3).

314 Our treatments had a greater impact on calcifying fluid chemistry (Figure 3).
315 pH_{cf}, estimated from $\delta^{11}B$, declined significantly with both decreasing seawater pH
316 and increasing seawater DIC for three of four species (Figure 4; Table S3; both corals
317 and *S. durum*). Ω of seawater did not affect pH_{cf} in any species. In the treatment with
318 similar Ω, pH_{cf} was mostly driven by seawater pH (highest pH_{cf} in the high seawater
319 pH).

320 We utilized aragonite-specific proxies to quantify the calcifying fluid DIC
321 (DIC_{cf}) of the two coral species. DIC_{cf} derived from B/Ca and $\delta^{11}B$ (Holcomb,
322 DeCarlo, Gaetani, & McCulloch, 2016; McCulloch, D'Olivo, Falter, Holcomb, &
323 Trotter, 2017) of both coral species was significantly positively correlated with
324 increasing DIC and decreasing pH in seawater (Figure 5a, Table S3). Seawater Ω did
325 not influenced DIC_{cf} in *A. yongei*. In the three treatments with similar Ω, DIC_{cf} was
326 the highest (and B/Ca the lowest for CCA) in the treatment with elevated DIC.

327 Calcifying fluid Ω_a derived from peak widths in Raman spectra (DeCarlo et
328 al., 2017) did not significantly change in response to seawater pH or DIC for either
329 coral species (Figure 6). It marginally decreased with seawater Ω for *P. damicornis*.
330 While there are no published data of B/Ca or Raman spectroscopy for abiogenic high-
331 Mg calcites, both have been interpreted as carbonate system proxies in CCA (Donald,
332 Ries, Stewart, Fowell, & Foster, 2017; Kamenos et al., 2013). We interpret B/Ca and
333 Raman spectra as indicative of calcifying fluid DIC and calcite saturation state ($\Omega_{Cal\ cf}$)
334 respectively (Figure 6) based on their systematics in aragonite. However, without
335 the abiogenic high-Mg calcite calibrations, we quantify the response of B/Ca and

Raman peak width directly, rather than converting them to carbonate system parameters as we can for the aragonitic corals. We therefore assume that there is both an inverse relationship between B/Ca and DIC_{cf}, and a positive relationship between FWHM and mineral-specific saturation state in the calcifying fluid, as is the case in aragonite precipitating from seawater-like solutions (Holcomb et al., 2016; DeCarlo et al., 2017). B/Ca of *S. durum* declined significantly (indicating a potential increase in DIC_{cf}) as seawater pH decreased and as seawater DIC increased (Figure 5; Table S3). B/Ca was lowest in *S. durum* in the High DIC – Low pH treatment, and highest in the Low DIC – High pH treatment (though the latter was not statistically different). This was the opposite trend of the pH_{cf}. Ω of seawater did not affect B/Ca of any species. Raman peak width significantly increased with seawater DIC for *Neogoniolithon* sp., but did not change with seawater treatments for *S. durum* (Figure 6).

We utilized Ω_{cf} and $[CO_3^{2-}]_{cf}$ estimates to calculate $[Ca^{2+}]_{cf}$ in the two coral species. There was a treatment effect on $[Ca^{2+}]_{cf}$ of *P. damicornis* (Table S2, Fig. S1), while $[Ca^{2+}]_{cf}$ of *A. yongei* was not affected. In *P. damicornis* $[Ca^{2+}]_{cf}$ was significantly elevated in the High DIC – Low pH treatment compared to most others.

Photosynthetic rates were only determined on the coral *A. yongei* and the coralline *S. durum*. Photosynthesis increased significantly with increasing DIC and decreasing pH for *A. yongei* (Fig. S2, Table S2). There was no relationship between photosynthesis and Ω for of *A. yongei*. Photosynthesis of *S. durum* was not affected by the treatments (Table S2) and was not correlated to any parameter of the carbonate chemistry (Fig. S2).

Discussion

Here we demonstrate that two coral and two coralline algal species have the ability to control their calcification physiology under a large range of carbonate chemistry conditions that extend well beyond their natural range. Even when calcifying fluid carbonate chemistry was altered by our treatments, this only translated to shifts in calcification rates for one of the four species. Seawater pH and DIC were the primary drivers of changes in calcifying fluid chemistry, not the saturation state of seawater. Our findings were highly similar for corals and coralline algae and can be summarized into two pathways via which the calcifying fluid is impacted by seawater

carbonate chemistry: 1) Seawater pH is the primary driver of changes in pH_{cf}; 2) seawater DIC is the primary driver of DIC_{cf} and can also influence pH_{cf}. Conversely, our Raman spectroscopy analyses indicate that three of the four species maintain a constant saturation state irrespective of the external seawater conditions, apart from *Neogonioltihon* sp., which exhibited a slight sensitivity to seawater DIC. This supports the notion that calcifiers must achieve threshold levels of Ω_{cf} for $CaCO_3$ precipitation, and suggests that both corals and CCA have the ability to manipulate their calcifying fluid chemistry to reach these species-specific Ω_{cf} thresholds when assessed over longer time periods, such as here. Notably, these results provide a mechanistic understanding of the resilience to ocean acidification found during *in situ* studies on coralline algae (Kamenos et al. 2016) and corals (Barkley et al. 2015, 2017) at naturally acidified sites.

Our results give support to some of the principles behind the $[DIC]/[H^+]$ hypothesis. However, the idea that $[DIC]/[H^+]$ ratios linearly drive calcification is also simplistic. This was also demonstrated in past $[Ca^{2+}]$ manipulation experiments that yielded treatments with similar $[DIC]/[H^+]$ ratios but different saturation states (Gattuso, Frankignoulle, Bourge, Romaine, & Buddemeier, 1998; Marshall & Clode, 2002). Calcification decreased under low $[Ca^{2+}]$ in these experiments despite $[DIC]/[H^+]$ ratios being at ambient levels. However, the role of calcium is complex because the decrease in calcification at lower $[Ca^{2+}]$ (and therefore Ω) could result from the disruption of the numerous physiological pathways in which $[Ca^{2+}]$ is involved. Furthermore, $[Ca^{2+}]$ is significantly (at least ten-fold) more abundant compared to $[CO_3^{2-}]$ in the oceans, and unlike $[CO_3^{2-}]$ will not be affected by OA. Our results also support the hypothesis that seawater $[DIC]/[H^+]$ ratios, and its covariate Ω, are not the sole driver of calcification. This is demonstrated by the different calcification rates, pH_{cf}, and DIC_{cf} measured in the three treatments where seawater Ω ($[DIC]/[H^+]$ ratios) were similar but [DIC] and pH differed. Thus, while seawater pH and DIC independently control the conditions within the calcifying fluid of all four species examined here, only pH was found to be the dominant driver of calcification. Furthermore, we also found that $[Ca^{2+}]_{cf}$ was increased well above seawater $[Ca^{2+}]$ only in *P. damicornis* in the treatment with the lowest pH_{cf}. This result suggest that upregulation of $[Ca^{2+}]_{cf}$ in some coral species (and possibly CCA) could be a mechanism that enables constant Ω_{cf} when pH_{cf} decreases (DeCarlo, Comeau,

Cornwall, & McCulloch, 2018). These results also suggest that the correlation between seawater saturation state and calcification measured during [Ca^{2+}] manipulations could have been the result of changes in [Ca^{2+}]$_{cf}$ caused by differences in seawater [Ca^{2+}] and not saturation state *per se*. However, further research is required to verify this.

Past attempts to disentangle the effects of different carbonate system parameters on calcification processes have been hampered by a number of limitations. The majority of the past studies that have aimed to separate the different parameters of the seawater carbonate chemistry are based on very short-term incubations where the organisms were exposed to the manipulated seawater only during the few hours necessary to perform the physiological measurements (Table S4). While those studies are valuable, they mainly provide information on shock responses of organisms not acclimated to the treatments. These treatments are often extremely different from seawater carbonate chemistry encountered previously by the organisms. The present study shows that organisms have a greater capacity over much longer time periods (8-13 weeks for corals and 21 weeks for CCA) to adjust the chemistry in their calcifying fluid and therefore maintain their calcification when exposed to a large range of conditions. This is especially demonstrated by the low correlation (R^2) between seawater carbonate chemistry and all the physiological parameters measured here. However, such adjustments require the involvement of physiological mechanisms (gene expressions for carbonic anhydrase, H^+/Ca^{2+} transporters, etc. (Zoccola et al., 2015) that necessitate time to be expressed. Another limitation of past studies was that conditions in the calcifying fluid were unknown (or only known in the growing margin for pH_{cf} (Comeau, Tambutté, et al., 2017), which did not allow past research to clearly establish the mechanisms responsible, beyond more easily measurable calcification and photosynthetic rates. Here, we overcome this problem by determining the relevant chemistry in the calcifying fluid for numerous taxa, and show that seawater pH and DIC differentially affect conditions in the calcifying fluid.

The magnitude of the effects of seawater carbonate chemistry on the different metabolic processes (pH_{cf}, DIC_{cf}, Ω_{cf}, photosynthesis and calcification) are species-specific, but the ability to achieve a threshold level of Ω_{cf} to maintain constant calcification is relatively consistent across taxa. For example, calcification rates of *P. damicornis* are known to be insensitive to low seawater pH (Comeau, Cornwall, &

McCulloch, 2017), while *Neogoniolithon* sp. calcification and pH_{cf} do not decline over larger ranges in seawater pH than examined here (i.e. to 7.64)(Cornwall et al., 2017). This is in contrast to more dramatic declines in calcification under OA observed for *A. yongei* or *S. durum*, particularly when pH is much lower than employed here (Comeau, Cornwall, & McCulloch, 2017; Cornwall, Comeau, & McCulloch, 2017). This suite of responses to seawater pH were repeated again here. However, while species-specific effects were observed, the general trends persisted across taxa. This indicates an evolutionary convergence of the calcification mechanisms of the two taxa (Scleractinian corals and Rhodophyte CCA), where organisms are able to control their pH_{cf}, DIC_{cf}, and $Ca^{2+}{}_{cf}$ to achieve a certain Ω_{cf} threshold necessary for calcification. For both taxa, organisms have developed the necessary physiological mechanisms (proton pumping, carbonic anhydrase, calcium pumping, etc.) to create internal conditions favorable for the mineralization process under a large range of external carbonate chemistry conditions. This is likely the result of the large past variations in oceanic carbonate chemistry conditions that these taxa evolved in. Over geological time, pH and DIC have been at levels even more extreme than that employed in our study (Hönisch et al., 2012).

It is not unexpected that pH and DIC in seawater are the main drivers of pH_{cf} and DIC_{cf} respectively. Declines in pH_{cf} as seawater pH decreases are species-specific, and sometimes result in concomitant drops in calcification rates (Cornwall et al., 2017; Holcomb et al., 2014; McCulloch et al., 2012; Venn et al., 2013). The fact that *P. damicornis* did not decrease its calcification with declining pH_{cf} supports past findings (Comeau, Cornwall, &McCulloch, 2017). Therefore, the fact that pH_{cf} is often impacted by seawater pH should not be taken as explicit evidence for the DIC/H^+ hypothesis. This is because changes in pH_{cf} do not always impact calcification rates. It is possible that declining seawater pH does not increase the energy required to export H^+ out of the calcifying fluid because pumping remains constant (M. McCulloch et al., 2012), and/or that other physiological mechanisms can counter declines in pH_{cf} for some species (e.g. increases in Ca^{2+} and DIC in the calcifying fluid). Additionally, the decrease in pH_{cf} with increasing seawater DIC found here is partly contradictory to results measured by confocal microscopy on the coral *S. pistillata* (Comeau, Tambutté, et al., 2017). It is possible that this is due to differences in treatments employed here, as the response to low DIC at ambient pH

was similar between studies. Another possibility is that the duration we used was sufficiently long to rule out shock responses that may have occurred in shorter term experiments (Table S4), or that the effects observed previously were species-specific.

When we compare the three treatments with constant pH, seawater DIC had a positive effect on *S. durum* and *A. yongei* calcification. A similar effect was observed in other species (corals *Porites rus*, *Stylophora pistilata* and *Madracis auretenra,* and the CCA *Porolithon onkodes*) which increased calcification under elevated DIC when pH was kept constant (Comeau, Tambutté, et al., 2017; Comeau et al., 2013; Jury et al., 2010; Marubini et al., 2008). However, here seawater DIC did not significantly affect calcification rates of CCA or corals when all the treatments were considered because of the larger effects of pH. While seawater DIC did not have a linear effect on calcification rates, we still consider it could be important in some circumstances. The elevation of DIC_{cf} compared to seawater, and increases in DIC_{cf} with seawater DIC, indicates that corals actively concentrate DIC in the calcifying fluid, but that this process is influenced by seawater [DIC]. Increasing DIC_{cf} could result from additional external DIC transported with seawater to the site of calcification (Gagnon, Adkins, & Erez, 2012), or from an increase of the active transport of bicarbonate using specific transporters (Zoccola et al., 2015). Additional DIC_{cf} could also be the result of increasing photosynthetic activity with seawater DIC measured in *A. yongei*. Increasing photosynthetic rates and metabolic activity could be associated with an increase in light respiration rates that would favor the transport of respiratory CO_2 to the site of calcification. The control of seawater DIC observed in coral DIC_{cf} were mirrored in the CCA B/Ca, likely indicative of consistent DIC_{cf} responses among corals and CCA.

In conclusion, we propose an alternate explanation to both the Ω and DIC/H^+ hypotheses regarding how seawater carbonate chemistry affects calcification processes based on our findings. Seawater pH ($[H^+]$) is the dominant driver of responses to OA, with [DIC] also playing a role. Instead of a linear relationship that correlates with Ω, $[H^+]$ and [DIC] have complex, independent, species-specific effects on calcification physiology, whereby pH_{cf} and DIC_{cf} are driven primarily by seawater pH and DIC respectively via the mechanisms discussed above. Marine calcifiers have therefore evolved to modulate their calcifying fluid pH, DIC and Ca^{2+} to achieve

certain Ω thresholds necessary to precipitate calcium carbonate under a large range of carbonate chemistry conditions.

Acknowledgements

B Moore, A-M Comeau-Nisumaa and V Schoepf provided vital laboratory support. MTM was supported by an ARC Laureate Fellowship (LF120100049), S. C. was supported by an ARC DECRA (DE160100668). The authors acknowledge the facilities, and the scientific and technical assistance of the Australian Microscopy & Microanalysis Research Facility at the Centre for Microscopy, Characterisation & Analysis, The University of Western Australia, a facility funded by the University, State and Commonwealth Governments.

Author contributions

SC, CEC, and MTM designed the research. SC and CEC wrote the paper. TMD and MTM edited the paper. SC, CEC and EK ran the experiment. SC, CEC, and TMD performed geochemical and statistical analysis.

References

Bach, L. T., Mackinder, L. C. M., Schulz, K. G., Wheeler, G., Schroeder, D. C., Brownlee, C., & Riebesell, U. (2013). Dissecting the impact of CO2 and pH on the mechanisms of photosynthesis and calcification in the coccolithophore Emiliania huxleyi. *The New Phytologist*, *199*(1), 121–134. https://doi.org/10.1111/nph.12225

Chan, N. C. S., & Connolly, S. R. (2013). Sensitivity of coral calcification to ocean acidification: a meta-analysis. *Global Change Biology*, *19*(1), 282–290. https://doi.org/10.1111/gcb.12011

Comeau, S., Carpenter, R. C., & Edmunds, P. J. (2013). Coral reef calcifiers buffer their response to ocean acidification using both bicarbonate and carbonate. *Proceedings of the Royal Society of London B: Biological Sciences*, *280*(1753), 20122374. https://doi.org/10.1098/rspb.2012.2374

Comeau, S., Cornwall, C. E., & McCulloch, M. T. (2017). Decoupling between the response of coral calcifying fluid pH and calcification to ocean acidification. *Scientific Reports*, *7*(1), 7573. https://doi.org/10.1038/s41598-017-08003-z

Comeau, S., Tambutté, E., Carpenter, R. C., Edmunds, P. J., Evensen, N. R., Allemand, D., … Venn, A. A. (2017). Coral calcifying fluid pH is modulated by seawater carbonate chemistry not solely seawater pH. *Proc. R. Soc. B*, *284*(1847), 20161669. https://doi.org/10.1098/rspb.2016.1669

Cornwall, C. E., Comeau, S., & McCulloch, M. T. (2017). Coralline algae elevate pH at the site of calcification under ocean acidification. *Global Change Biology*, n/a-n/a. https://doi.org/10.1111/gcb.13673

Cornwall, C. E., & Hurd, C. L. (2016). Experimental design in ocean acidification research: problems and solutions. *ICES Journal of Marine Science*, *73*(3), 572–581. https://doi.org/10.1093/icesjms/fsv118

DeCarlo, T. M., Comeau, S., Cornwall, C. E., & McCulloch, M. T. (2018). Coral resistance to ocean acidification linked to increased calcium at the site of

calcification. *Proc. R. Soc. B*, *285*(1878), 20180564. https://doi.org/10.1098/rspb.2018.0564

DeCarlo, T. M., D'Olivo, J. P., Foster, T., Holcomb, M., Becker, T., & McCulloch, M. T. (2017). Coral calcifying fluid aragonite saturation states derived from Raman spectroscopy. *Biogeosciences*, *14*(22), 5253–5269. https://doi.org/10.5194/bg-14-5253-2017

Dickson, A. G., Sabine, C. L., & Christian, J. R. (2007). *Guide to best practices for Ocean CO2 measurements*. (PICES Special Publication, Vol. 3).

Donald, H. K., Ries, J. B., Stewart, J. A., Fowell, S. E., & Foster, G. L. (2017). Boron isotope sensitivity to seawater pH change in a species of Neogoniolithon coralline red alga. *Geochimica et Cosmochimica Acta*, *217*, 240–253. https://doi.org/10.1016/j.gca.2017.08.021

Foster, G. L., Pogge von Strandmann, P. a. E., & Rae, J. W. B. (2010). Boron and magnesium isotopic composition of seawater. *Geochemistry, Geophysics, Geosystems*, *11*(8), Q08015. https://doi.org/10.1029/2010GC003201

Furla, P., Galgani, I., Durand, I., & Allemand, D. (2000). Sources and mechanisms of inorganic carbon transport for coral calcification and photosynthesis. *The Journal of Experimental Biology*, *203*(Pt 22), 3445–3457.

Gagnon, A. C., Adkins, J. F., & Erez, J. (2012). Seawater transport during coral biomineralization. *Earth and Planetary Science Letters*, *329–330*, 150–161. https://doi.org/10.1016/j.epsl.2012.03.005

Gattuso, J.-P., Frankignoulle, M., Bourge, I., Romaine, S., & Buddemeier, R. W. (1998). Effect of calcium carbonate saturation of seawater on coral calcification. *Global and Planetary Change*, *18*(1), 37–46. https://doi.org/10.1016/S0921-8181(98)00035-6

Herfort, L., Thake, B., & Taubner, I. (2008). Bicarbonate Stimulation of Calcification and Photosynthesis in Two Hermatypic Corals(1). *Journal of Phycology*, *44*(1), 91–98. https://doi.org/10.1111/j.1529-8817.2007.00445.x

572 Holcomb, M., DeCarlo, T. M., Gaetani, G. A., & McCulloch, M. (2016). Factors
573 affecting B/Ca ratios in synthetic aragonite. *Chemical Geology*, *437*, 67–76.
574 https://doi.org/10.1016/j.chemgeo.2016.05.007
575 Holcomb, M., Venn, A. A., Tambutté, E., Tambutté, S., Allemand, D., Trotter, J., &
576 McCulloch, M. (2014). Coral calcifying fluid pH dictates response to ocean
577 acidification. *Scientific Reports*, *4*, 5207. https://doi.org/10.1038/srep05207
578 Hönisch, B., Ridgwell, A., Schmidt, D. N., Thomas, E., Gibbs, S. J., Sluijs, A., …
579 Williams, B. (2012). The Geological Record of Ocean Acidification. *Science*,
580 *335*(6072), 1058–1063. https://doi.org/10.1126/science.1208277
581 Jokiel, P. L. (2013). Coral reef calcification: carbonate, bicarbonate and proton flux
582 under conditions of increasing ocean acidification. *Proceedings. Biological*
583 *Sciences*, *280*(1764), 20130031. https://doi.org/10.1098/rspb.2013.0031
584 Jokiel, Paul Louis. (2011). Ocean Acidification and Control of Reef Coral
585 Calcification by Boundary Layer Limitation of Proton Flux. *Bulletin of*
586 *Marine Science*, *87*(3), 639–657. https://doi.org/10.5343/bms.2010.1107
587 Jury, C. P., Whitehead, R. F., & Szmant, A. M. (2010). Effects of variations in
588 carbonate chemistry on the calcification rates of Madracis auretenra (=
589 Madracis mirabilis sensu Wells, 1973): bicarbonate concentrations best predict
590 calcification rates. *Global Change Biology*, *16*(5), 1632–1644.
591 https://doi.org/10.1111/j.1365-2486.2009.02057.x
592 Kamenos, N. A., Perna, G., Gambi, M. C., Micheli, F., & Kroeker, K. J. (2016).
593 Coralline algae in a naturally acidified ecosystem persist by maintaining
594 control of skeletal mineralogy and size. *Proc. R. Soc. B*, *283*(1840), 20161159.
595 https://doi.org/10.1098/rspb.2016.1159
596 Kamenos, Nicholas A., Burdett, H. L., Aloisio, E., Findlay, H. S., Martin, S.,
597 Longbone, C., … Calosi, P. (2013). Coralline algal structure is more sensitive
598 to rate, rather than the magnitude, of ocean acidification. *Global Change*
599 *Biology*, *19*(12), 3621–3628. https://doi.org/10.1111/gcb.12351

Klochko, K., Kaufman, A. J., Yao, W., Byrne, R. H., & Tossell, J. A. (2006). Experimental measurement of boron isotope fractionation in seawater. *Earth and Planetary Science Letters*, *248*(1–2), 276–285. https://doi.org/10.1016/j.epsl.2006.05.034

Kroeker, K. J., Kordas, R. L., Crim, R. N., & Singh, G. G. (2010). Meta-analysis reveals negative yet variable effects of ocean acidification on marine organisms. *Ecology Letters*, *13*(11), 1419–1434. https://doi.org/10.1111/j.1461-0248.2010.01518.x

Marshall, A. T., & Clode, P. L. (2002). Effect of increased calcium concentration in sea water on calcification and photosynthesis in the scleractinian coral Galaxea fascicularis. *The Journal of Experimental Biology*, *205*(Pt 14), 2107–2113.

Marubini, F., Ferrier-Pagès, C., Furla, P., & Allemand, D. (2008). Coral calcification responds to seawater acidification: a working hypothesis towards a physiological mechanism. *Coral Reefs*, *27*(3), 491–499. https://doi.org/10.1007/s00338-008-0375-6

Marubini, Francesca, Ferrier-Pages, C., & Cuif, J.-P. (2003). Suppression of skeletal growth in scleractinian corals by decreasing ambient carbonate-ion concentration: a cross-family comparison. *Proceedings. Biological Sciences*, *270*(1511), 179–184. https://doi.org/10.1098/rspb.2002.2212

McCoy, S. J., & Kamenos, N. A. (2015). Coralline algae (Rhodophyta) in a changing world: integrating ecological, physiological, and geochemical responses to global change. *Journal of Phycology*, *51*(1), 6–24. https://doi.org/10.1111/jpy.12262

McCulloch, M., Falter, J., Trotter, J., & Montagna, P. (2012). Coral resilience to ocean acidification and global warming through pH up-regulation. *Nature Climate Change*, *2*(8), 623–627. https://doi.org/10.1038/nclimate1473

McCulloch, M. T., D'Olivo, J. P., Falter, J., Holcomb, M., & Trotter, J. A. (2017). Coral calcification in a changing World and the interactive dynamics of pH

and DIC upregulation. *Nature Communications*, *8*, 15686. https://doi.org/10.1038/ncomms15686

Pauly, M., Kamenos, N. A., Donohue, P., & LeDrew, E. (2015). Coralline algal Mg-O bond strength as a marine pCO2 proxy. *Geology*, *43*(3), 267–270. https://doi.org/10.1130/G36386.1

Perrin, J., Vielzeuf, D., Laporte, D., Ricolleau, A., Rossman, G. R., & Floquet, N. (2016). Raman characterization of synthetic magnesian calcites. *American Mineralogist*, *101*(11), 2525–2538. https://doi.org/10.2138/am-2016-5714

Ross, C. L., Falter, J. L., Schoepf, V., & McCulloch, M. T. (2015). Perennial growth of hermatypic corals at Rottnest Island, Western Australia (32°S). *PeerJ*, *3*, e781. https://doi.org/10.7717/peerj.781

Schneider, K., & Erez, J. (2006). The effect of carbonate chemistry on calcification and photosynthesis in the hermatypic coral Acropora eurystoma. *Limnology and Oceanography*, *51*(3), 1284–1293. https://doi.org/10.4319/lo.2006.51.3.1284

Trotter, J., Montagna, P., McCulloch, M., Silenzi, S., Reynaud, S., Mortimer, G., … Rodolfo-Metalpa, R. (2011). Quantifying the pH 'vital effect' in the temperate zooxanthellate coral Cladocora caespitosa: Validation of the boron seawater pH proxy. *Earth and Planetary Science Letters*, *303*(3–4), 163–173. https://doi.org/10.1016/j.epsl.2011.01.030

Urmos, J., Sharma, S. K., & Mackenzie, F. T. (1991). Characterization of some biogenic carbonates with Raman spectroscopy. *American Mineralogist*, *76*(3–4), 641–646.

Venn, A. A., Tambutté, E., Holcomb, M., Laurent, J., Allemand, D., & Tambutté, S. (2013). Impact of seawater acidification on pH at the tissue–skeleton interface and calcification in reef corals. *Proceedings of the National Academy of Sciences*, *110*(5), 1634–1639. https://doi.org/10.1073/pnas.1216153110

Zoccola, D., Ganot, P., Bertucci, A., Caminiti-Segonds, N., Techer, N., Voolstra, C. R., … Tambutté, S. (2015). Bicarbonate transporters in corals point towards a

key step in the evolution of cnidarian calcification. *Scientific Reports*, *5*.
https://doi.org/10.1038/srep09983

662 **Figures Legend**
663
664 **Fig. 1.** The two corals (*Acropora yongei* and *Pocillopora damicornis*) and the two
665 crustose coralline algae (*Neogoniolithon* sp. and *Sporolithon durum*) were incubated
666 under five seawater treatments obtained by manipulating pH_T and the dissolved
667 inorganic carbon concentration [DIC]. Here we employ treatments with similar DIC
668 and different pH and Ω, similar pH with different DIC and Ω, and similar Ω with
669 different pH and DIC. These treatment combinations allow us to separate out the
670 effects of seawater DIC, pH and Ω, without the need for additional treatments. The
671 shade of greys represents the seawater aragonite saturation state.
672
673 **Fig. 2.** Effects of seawater DIC, pH_T and saturation state on the surface area-
674 normalized net calcification of the tested organisms. The first row shows calcification
675 for the coral *Acropora yongei* (circles) and *Pocillopora damicornis* (squares). The
676 second row shows calcification for the coralline algae *Neogoniolithon* sp. (triangles)
677 and *Sporolithon durum* (diamonds). The colors represent the different treatments:
678 Low DIC-High pH (dark green), Low DIC-Ambient pH (light green), Ambient (blue),
679 High DIC-Low pH (orange), and High DIC – Ambient pH (red). See Fig. 1 for
680 treatment seawater carbonate chemistry. The dotted line represents the linear
681 relationship with a significant slope p-value.
682
683 **Fig. 3.** Proportions of the variation (R^2) of the estimated variables explained by
684 seawater DIC (green), pH (red) and saturation state (blue) in multiple linear
685 regressions on calcification, pH in the calcifying fluid (pH_{cf}), dissolved inorganic
686 carbon in the calcifying fluid (DIC_{cf}), aragonite saturation state in the calcifying fluid
687 (Ω_{cf}), and a proxy for calcite saturation state in the calcifying fluid (FWHM). The
688 photos show the organisms used during the experiment.
689
690 **Fig. 4.** Estimates of pH in the calcifying fluid (pH_{cf}) obtained using $\delta^{11}B$. The first
691 row shows pH_{cf} determined on the coral *Acropora yongei* (circles) and *Pocillopora*
692 *damicornis* (squares) as a function of seawater DIC, pH and aragonite saturation state.
693 The second row shows pH_{cf} determined on the crustose coralline algae
694 *Neogoniolithon* sp. (triangles) and *Sporolithon durum* (diamonds). The colors
695 represent the different treatments: Low DIC-High pH (dark green), Low DIC-

Ambient pH (light green), Ambient (blue), High DIC-Low pH (orange), and High DIC – Ambient pH (red). The dotted lines represent the linear relationships with significant slope p-value.

Fig. 5. Estimates of DIC_{cf} (based on $\delta^{11}B$ and B/Ca ratios) for the coral *Acropora yongei* (circles) and *Pocillopora damicornis* (squares) and measured B/Ca ratios ($\mu mol\ mol^{-1}$) for the crustose coralline algae *Neogoniolithon* sp. (triangles) and *Sporolithon durum* (diamonds). The colors represent the different treatments: Low DIC-High pH (dark green), Low DIC-Ambient pH (light green), Ambient (blue), High DIC-Low pH (orange), and High DIC – Ambient pH (red). The dotted lines represent the relationships with significant slope p-value.

Fig. 6. Estimates of corals calcifying fluid Ω_{ar} and coralline algae FWHM (indicating the calcifying fluid Ω_{cal}) obtained using Raman spectroscopy. Measurements were done on the coral *Acropora yongei* (circles) and *Pocillopora damicornis* (squares) and the crustose coralline algae *Neogoniolithon* sp. (triangles) and *Sporolithon durum* (diamonds). The colors represent the different treatments: Low DIC-High pH (dark green), Low DIC-Ambient pH (light green), Ambient (blue), High DIC-Low pH (orange), and High DIC – Ambient pH (red).

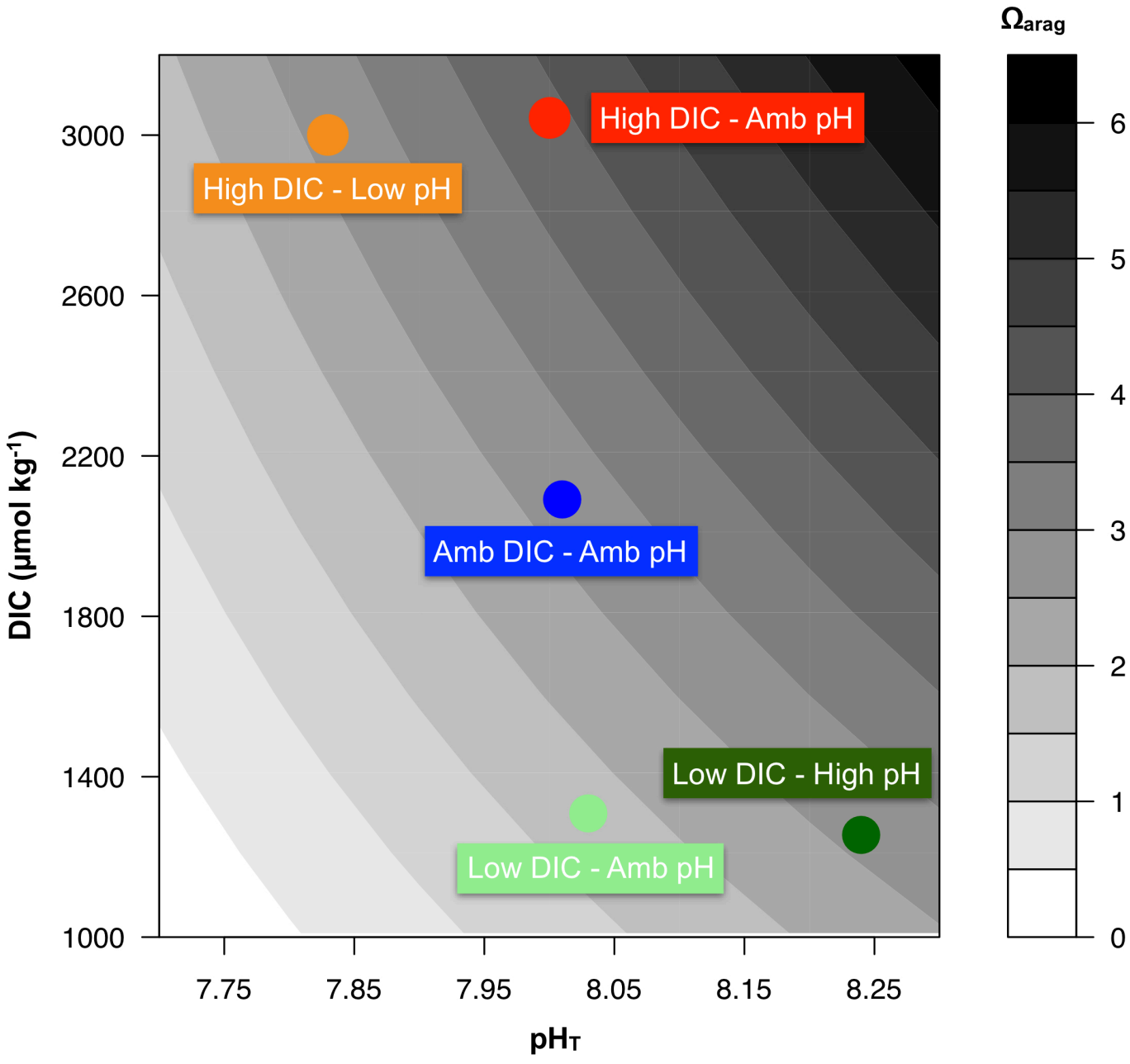
Ωarag
High DIC - Amb pH
High DIC - Low pH
Amb DIC - Amb pH
Low DIC - High pH
Low DIC - Amb pH
DIC (µmol kg-1)
3000
2600
2200
1800
1400
1000
7.75
7.85
7.95
8.05
8.15
8.25
pHT
6
5
4
3
2
1
0

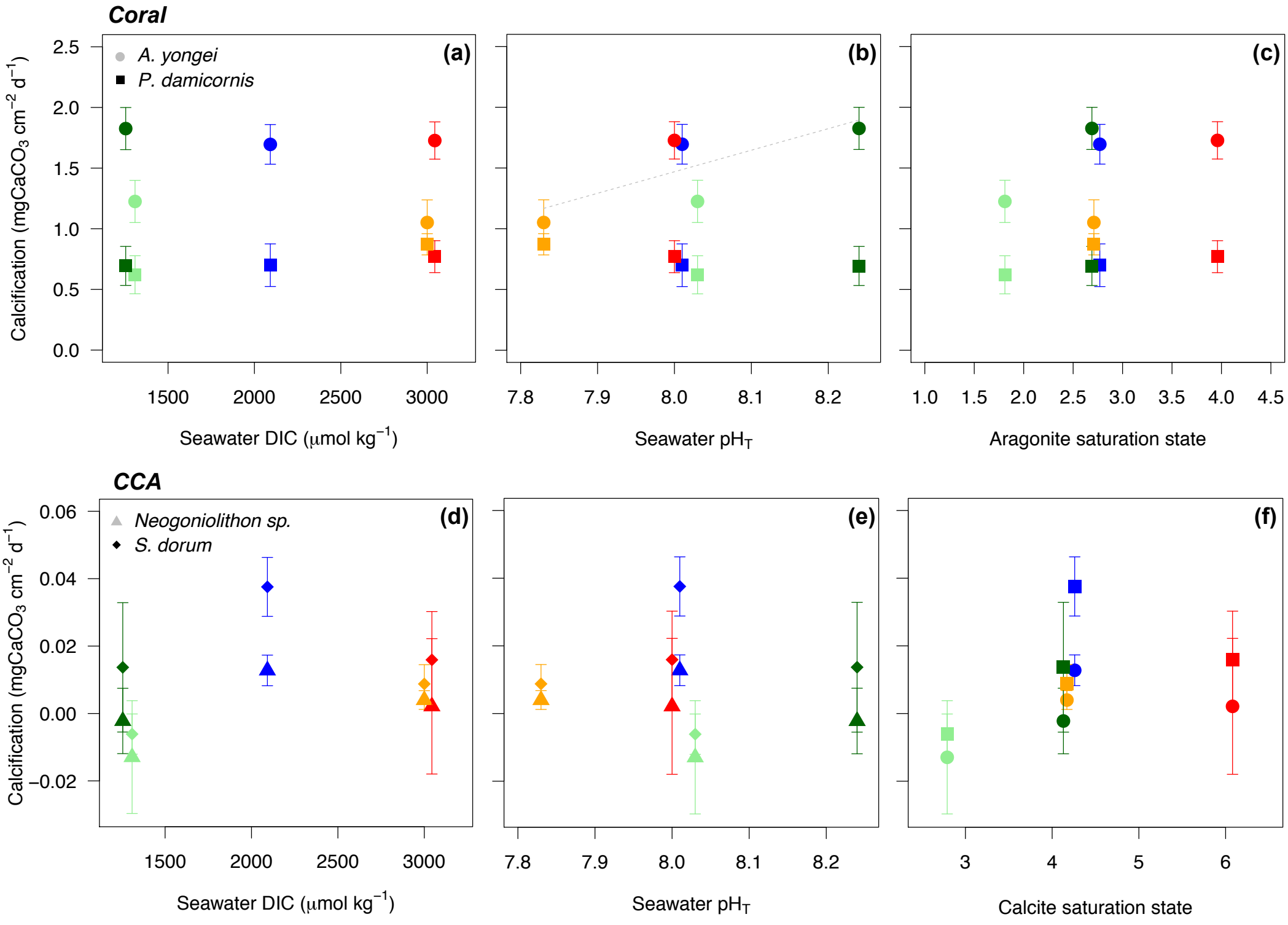
Coral
A. yongei
P. damicornis
(a)
(b)
(c)
Calcification (mgCaCO3 cm−2 d−1)
2.5
2.0
1.5
1.0
0.5
0.0
1500
2000
2500
3000
Seawater DIC (μmol kg−1)
7.8
7.9
8.0
8.1
8.2
Seawater pHT
1.0
1.5
2.0
2.5
3.0
3.5
4.0
4.5
Aragonite saturation state
CCA
Neogoniolithon sp.
S. dorum
(d)
(e)
(f)
Calcification (mgCaCO3 cm−2 d−1)
0.06
0.04
0.02
0.00
−0.02
1500
2000
2500
3000
Seawater DIC (μmol kg−1)
7.8
7.9
8.0
8.1
8.2
Seawater pHT
3
4
5
6
Calcite saturation state


10 cm
Acropora yongei


10 cm
Pocillopora damicornis

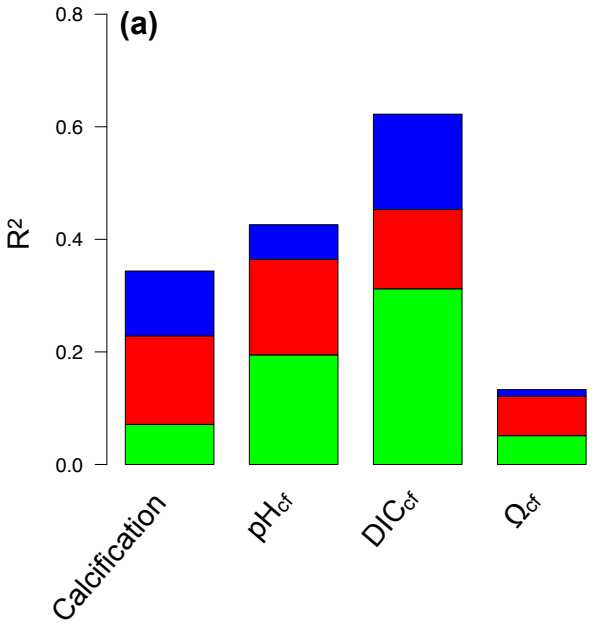
(a)
R2
0.8
0.6
0.4
0.2
0.0
Calcification
pHcf
DICcf
Ωcf

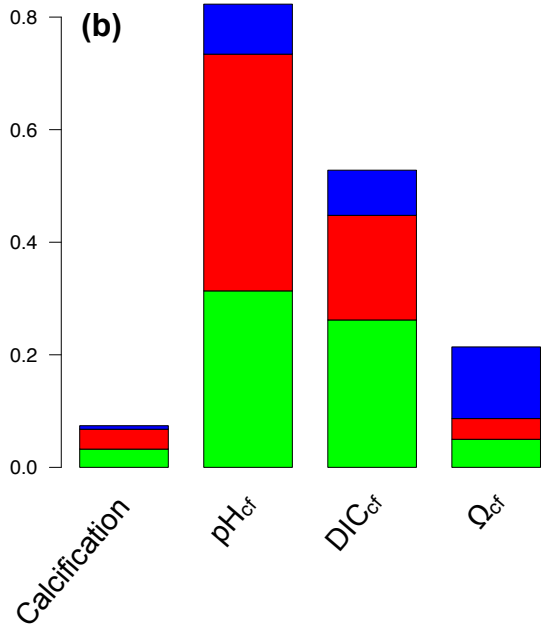
(b)
0.8
0.6
0.4
0.2
0.0
Calcification
pHcf
DICcf
Ωcf


1 cm
Neogoniolithon sp.


1 cm
Sporolithon durum

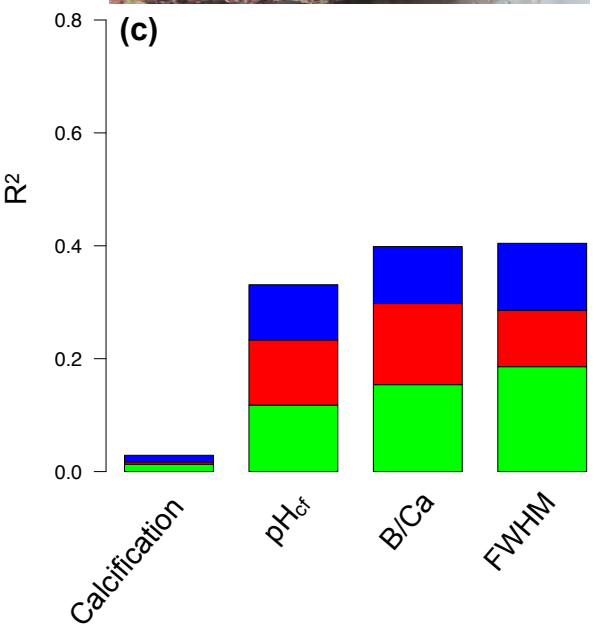
(c)
R2
0.8
0.6
0.4
0.2
0.0
Calcification
pHcf
B/Ca
FWHM

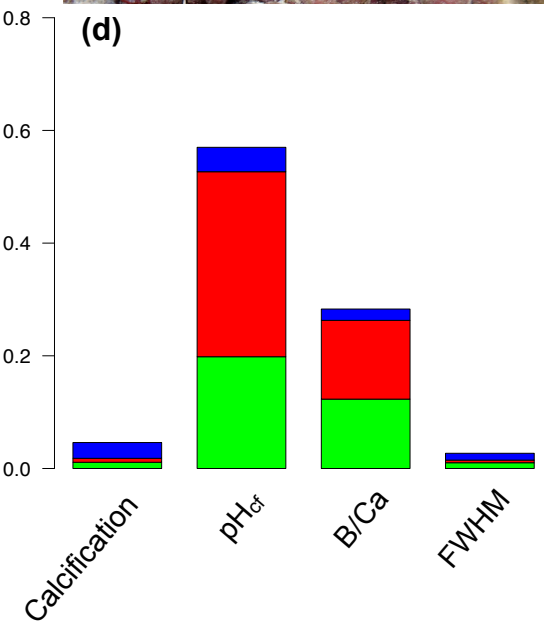
(d)
0.8
0.6
0.4
0.2
0.0
Calcification
pHcf
B/Ca
FWHM

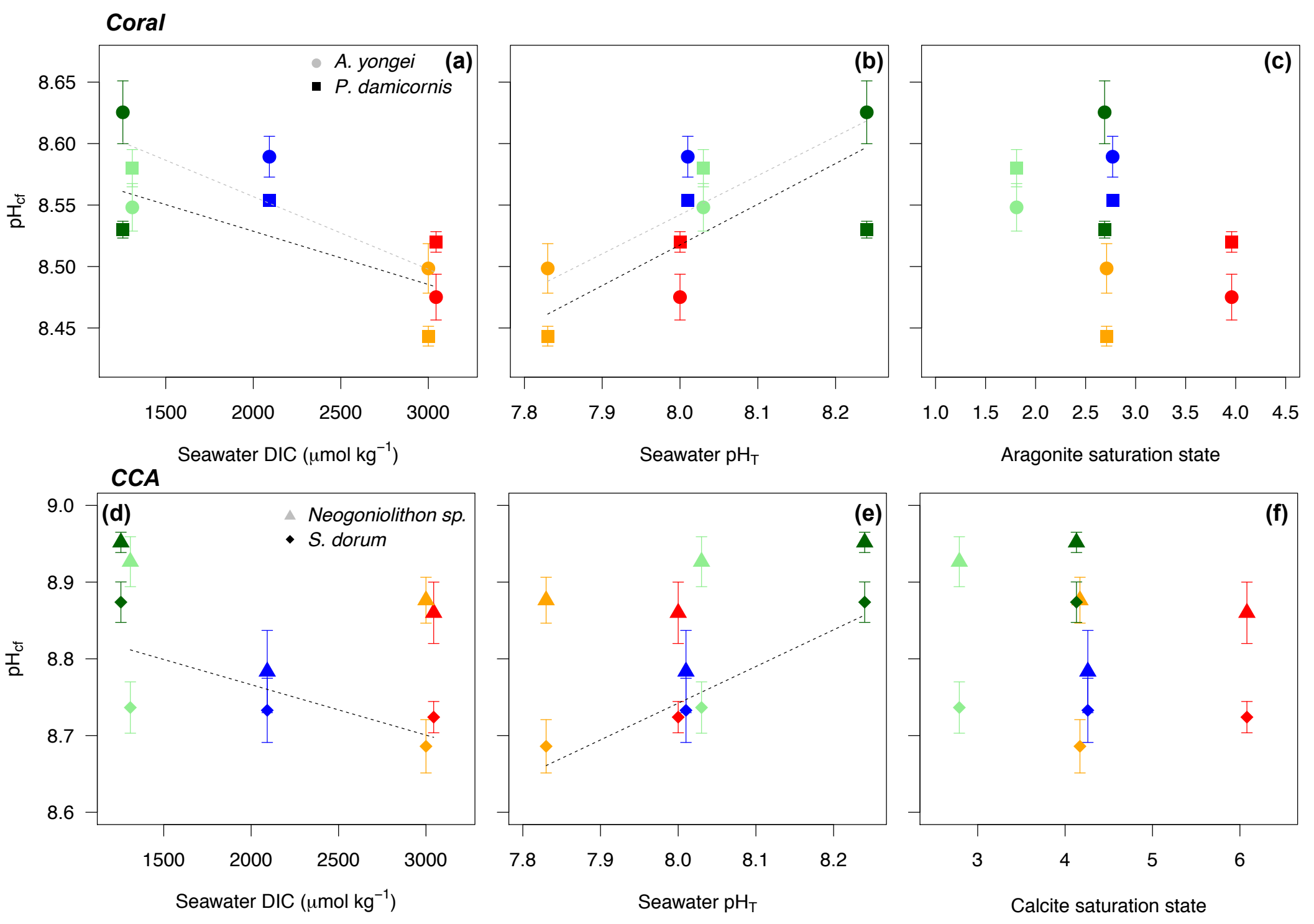
Coral
A. yongei
P. damicornis
(a)
(b)
(c)
pHcf
8.65
8.60
8.55
8.50
8.45
1500
2000
2500
3000
Seawater DIC (μmol kg−1)
7.8
7.9
8.0
8.1
8.2
Seawater pHT
1.0
1.5
2.0
2.5
3.0
3.5
4.0
4.5
Aragonite saturation state
CCA
Neogoniolithon sp.
S. dorum
(d)
(e)
(f)
9.0
8.9
8.8
8.7
8.6
3
4
5
6
Calcite saturation state

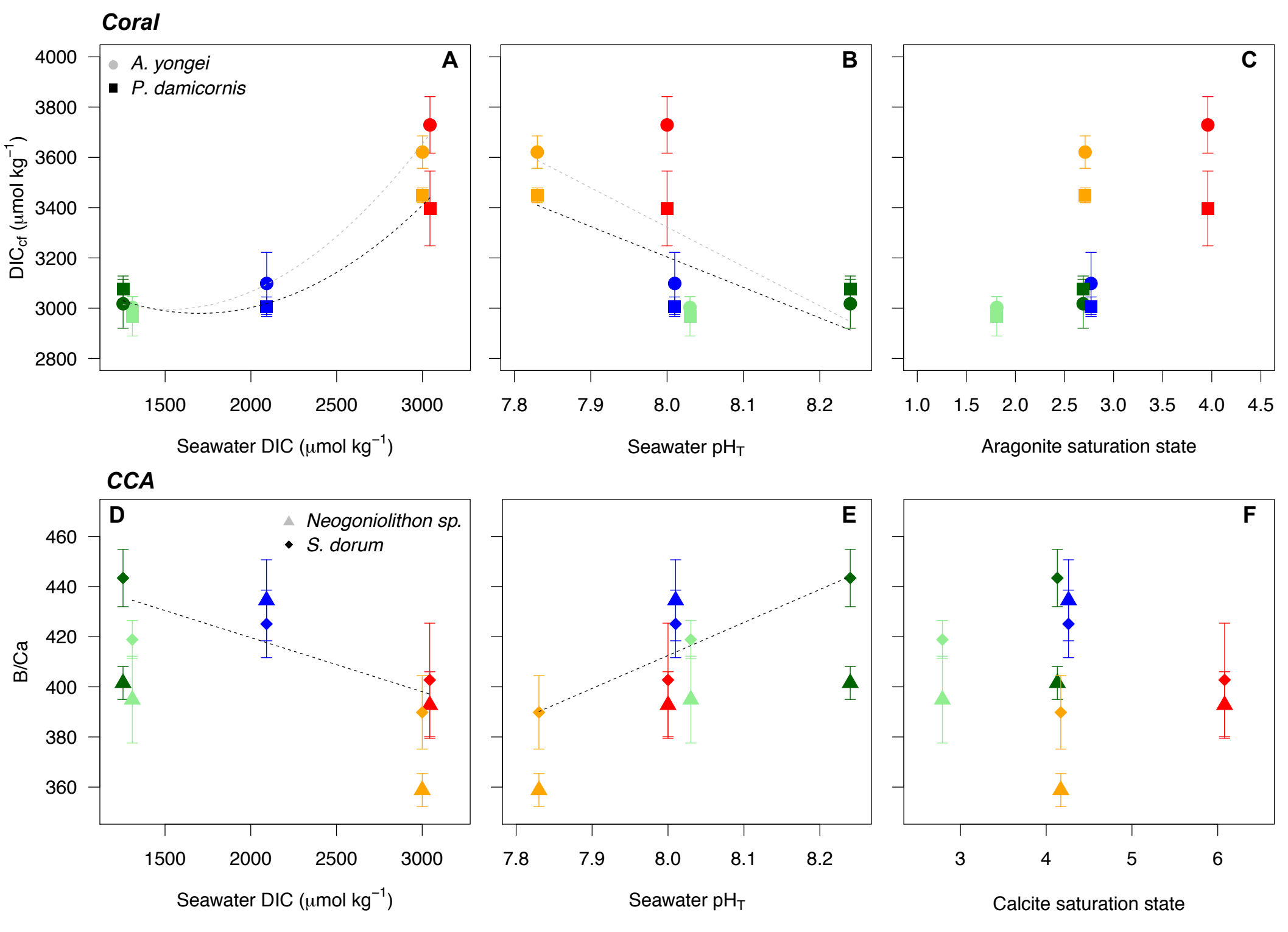
Coral
A
B
C
A. yongei
P. damicornis
DIC$_{cf}$ (μmol kg^{-1})
4000
3800
3600
3400
3200
3000
2800
1500
2000
2500
3000
Seawater DIC (μmol kg^{-1})
7.8
7.9
8.0
8.1
8.2
Seawater pH$_T$
1.0
1.5
2.0
2.5
3.0
3.5
4.0
4.5
Aragonite saturation state
CCA
D
E
F
Neogoniolithon sp.
S. dorum
B/Ca
460
440
420
400
380
360
1500
2000
2500
3000
Seawater DIC (μmol kg^{-1})
7.8
7.9
8.0
8.1
8.2
Seawater pH$_T$
3
4
5
6
Calcite saturation state

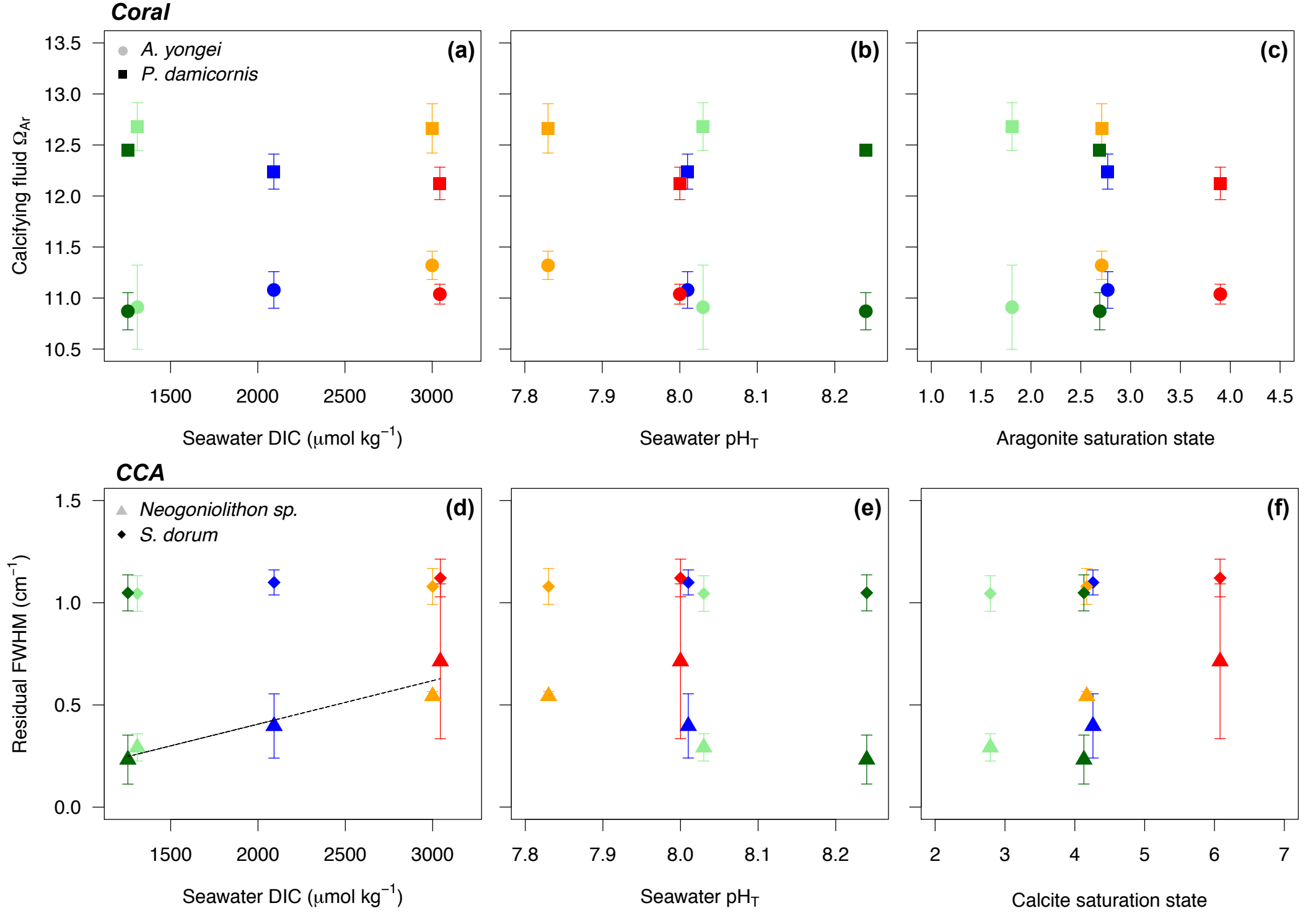
Coral
A. yongei
P. damicornis
(a)
(b)
(c)
Calcifying fluid Ω_{Ar}
13.5
13.0
12.5
12.0
11.5
11.0
10.5
1500
2000
2500
3000
Seawater DIC (μmol kg^{-1})
7.8
7.9
8.0
8.1
8.2
Seawater pH$_T$
1.0
1.5
2.0
2.5
3.0
3.5
4.0
4.5
Aragonite saturation state
CCA
Neogoniolithon sp.
S. dorum
(d)
(e)
(f)
Residual FWHM (cm^{-1})
1.5
1.0
0.5
0.0
1500
2000
2500
3000
Seawater DIC (μmol kg^{-1})
7.8
7.9
8.0
8.1
8.2
Seawater pH$_T$
2
3
4
5
6
7
Calcite saturation state

Supplementary Table 1: Mean carbonate chemistry in the incubations tanks. Dissolved inorganic carbon (DIC), pCO_2, and the saturation state of aragonite and calcite were calculated using measured pH_T, total alkalinity (A_T), temperature, and a salinity of 35.2 (SE < 0.1).

Treatment	**pH_T**	**DIC** (µmol kg^{-1})	**A_T** (µmol kg^{-1})	**pCO_2** (µatm)	**T** (°C)	**Ω_{arag}**	**Ω_{Cal}**
Ambient	8.01 ± 0.01	2092 ± 8	2339 ± 7	449 ± 12	20.4 ± 0.1	2.78 ± 0.05	4.28 ± 0.08
High DIC-Amb pH	8.00 ± 0.01	3044 ± 26.9	3356 ± 27	687 ± 27	20.5 ± 0.1	3.93 ± 0.10	6.05 ± 0.17
High DIC-Low pH	7.83 ± 0.01	3000 ± 19	3201 ± 23	1007 ± 30	20.6 ± 0.1	2.71 ± 0.06	4.17 ± 0.10
Low DIC-Amb pH	8.03 ± 0.01	1309 ± 10	1504 ± 9	267 ± 9	20.5 ± 0.1	1.83 ± 0.03	2.81 ± 0.06
Low DIC-High pH	8.24 ± 0.01	1255 ± 14	1549 ± 14	150 ± 5	20.6 ± 0.1	2.69 ± 0.04	4.15 ± 0.07

Supplementary Table 2. Summary of the ANOVA examining the effects of seawater treatments on the calcification, pH_{cf}, $DIC_{cf,}$ (B/Ca for the coralline algae) and Ω_{cf} (FWHM for the coralline algae). Post hoc results shows the significant differences between the treatments with L_DH_P = Low DIC-High pH, L_DA_P = Low DIC-Ambient pH, A = Ambient, H_DL_P = High DIC-Low pH, and H_DA_P = High DIC – Ambient pH.

Species	Physiological parameter	dF	F	p-value	Post-hoc
Acropora	Calcification	4,26	4.07	**0.010**	L_DH_P>H_DL_P
	pH_{cf}	4,26	9.39	**<0.001**	L_DH_P = A >H_DL_P = H_DA_P
	DIC_{cf}	4,26	13.75	**<0.001**	H_DL_P = H_DA_P > A= L_DH_P = L_DA_P
	Ω_{cf}	4,26	1.094	0.380	
	Ca_{cf}	4, 26	1.946	0.134	
	Photosynthesis	4,26	6.473	**0.001**	H_DL_P > L_DA_P = L_DH_P
Pocillopora	Calcification	4,22	0.449	0.772	
	pH_{cf}	4,22	33.88	**<0.001**	L_DH_P > L_DA_P = A = H_DA_P > H_DL_P
	DIC_{cf}	4,22	8.69	**<0.001**	H_DA_P = H_DL_P > A = L_DH_P = L_DA_P
	Ω_{cf}	4,25	1.83	0.154	
	Ca_{cf}	4, 22	6.172	**0.002**	H_DL_P > A = H_DA_P = L_DH_P
Neogoniolithon	Calcification	4,17	0.443	0.776	
	pH_{cf}	4,10	3.329	0.056	
	B/Ca	4,10	3.609	**0.045**	H_DL_P >A
	FWHM	4,8	1.433	0.307	
Sporolithon	Calcification	4,19	1.276	0.312	
	pH_{cf}	4,20	6.315	**0.002**	L_DH_P > A = H_DA_P = L_DH_P = L_DA_P
	B/Ca	4,20	2.039	0.129	
	FWHM	4,20	0.147	0.962	
	Photosynthesis	4,15	1.003	0.436	

Supplementary Table 3. Linear regressions with p-value of the slopes < 0.05. P values < 0.017 bolded based on Bonferroni corrections. Only parameters that describe more than 10 % of the variability are listed

Species	**Physiological parameter**	**Seawater parameter**	**Equation**	**Slope p-value**	**R^2**
Acropora	Calcification	pH	Y= -12.7 +1.77 x	**0.008**	**0.21**
		Ω_{arag}	Y = 1.24 + 0.08 x	0.034	0.14
	pH_{cf}	DIC	Y = 8.68 -5.91 10^{-5} x	**<0.001**	**0.40**
		pH	Y = 6.0 + 0.32 x	**<0.001**	**0.33**
		Ω_{arag}	Y = 8.65 -0.04 x	0.05	0.12
	DIC_{cf}	DIC	Y = 2461 + 0.38 x	**<0.001**	**0.61**
		pH	Y = 15846 -1565 x	**0.002**	**0.29**
	Photosynthesis	DIC	Y = 12.0 + 0.01 x	**0.002**	**0.28**
		pH	Y = 492.4 -57.6 x	**<0.001**	**0.32**
Pocillopora	pH_{cf}	DIC	8.62 – 4.3 x	**<0.001**	**0.45**
		pH	Y = 5.87 +0.33 x	**<0.001**	**0.73**
	DIC_{cf}	DIC	2687 + 0.23 x	**<0.001**	**0.5**
		pH	12894 - 1211 x	**<0.001**	**0.37**
		Ω_{arag}	2777 + 148 x	0.044	0.15
	Ω_{cf}	Ω_{arag}	Y = 13.19-0.27 x	0.034	0.15
Sporolithon	pH_{cf}	DIC	8.90 – 6.57 10-5 x	**0.003**	**0.32**
		pH	4.92 + 0.48 x	**<0.001**	**0.53**
	B/Ca	DIC	463 -0.02 x	**0.017**	**0.23**
		pH	-640 + 132 x	**0.010**	**0.27**
Neogoniolithon	FWHM	DIC	-1.90 + 2.13 x	0.024	0.38

Supplementary Table 4. Summary of the studies that have manipulated the carbonate chemistry to isolate the effect of species of the carbonate system on the physiology of corals and coralline algae.

Study	Species	Time in the treatment	Main driver	Physiological parameter	Manipulation
Gattuso et al. 1998[21]	*Acropora* *S. pisitillata*	2.5 hours	Ω	Calcification	Ca^{2+}
Marshall and Clode 2002[22]	*Galaxea fascicularis*	4 hours	Ω	Calcification	Ca^{2+}
Schneider and Erez 2006[15]	*Acropora eurystoma*	1- 2 hours	Ω /CO_3^{2-}	Calcification	A_T and pH
Schneider and Erez 2006[15]	*Acropora eurystoma*	1- 2 hours	none	Photosynthesis Respiration	A_T and pH
Marubini et al. 2008[13]	*S. pisitillata*	8 days	pH Ω	Calcification	A_T and pH
Marubini et al. 2008[13]	*S. pisitillata*	8 days	HCO_3^-	Photosynthesis	A_T and pH
Jury et al. 2010[12]	*M. auretenra*	2 hours	HCO_3^-	Calcification	A_T and pH
Herfort et al. 2008[11]	*P. porites* *Acropora*	0.5 hours	HCO_3^-	Calcification Photosynthesis	HCO_3^- addition
Comeau et al. 2013[10]	*P. rus*	2 weeks	$HCO_3^-$and CO_3^{2-}, Ω - DIC/H+	Calcification	A_T and pH
Comeau et al. 2013[10]	*P. onkodes*	2 weeks	$HCO_3^-$and CO_3^{2-}, Ω - DIC/H+	Calcification	A_T and pH
Comeau et al. 2017[9]	*S. pistillata*	2 weeks	CO_3^{2-}, Ω - DIC/H+	Calcification, pH_{cf}, photosynthesis	A_T and pH
Present	*A. yongei*	8 weeks	pH	Calcification	A_T and pH
Present	*A. yongei* *P. damicornis*	8 -13 weeks	pH	pH_{cf} DIC_{cf}	A_T and pH
Present	*A. yongei* *P. damicornis*	8 -13 weeks	DIC	DIC_{cf} pH_{cf} Photosynthesis	A_T and pH
Present	*P. damicornis*	13 weeks	none	Calcification	A_T and pH
Present	*A. yongei* *P. damicornis*	8 - 13 weeks	none	Ω_{cf}	A_T and pH
Present	*Neogoniolithon* *S. durum*	21 weeks	none	Calcification Photosynthesis	A_T and pH

Present	*S. durum*	21	weeks	pH	DIC_{cf} pH_{cf}	A_T and pH
Present	*S. durum*	21	weeks	DIC	DIC_{cf} pH_{cf}	A_T and pH
Present	*Neogoniolithon*	21	weeks	DIC	FWHM/Ω_{cf}	A_T and pH
Present	*S. durum*	21	weeks	none	FWHM/Ω_{cf}	A_T and pH

Fig. S1. Estimates of corals calcifying fluid [Ca^{2+}] (mean ± SE, n = 5 or 6) relative to seawater [Ca^{2+}]. Estimates were calculated for the coral *Acropora yongei* (circles) and *Pocillopora damicornis* (squares). The colors represent the different treatments: Low DIC-High pH (dark green), Low DIC-Ambient pH (light green), Ambient (blue), High DIC-Low pH (orange), and High DIC – Ambient pH (red).

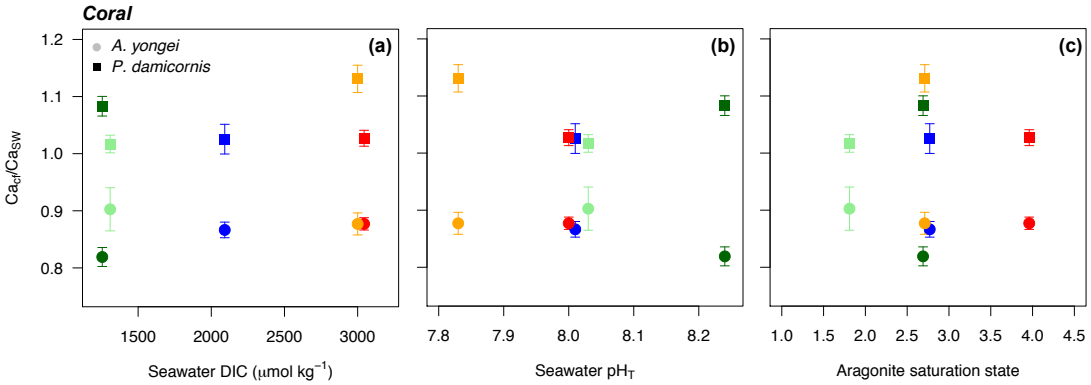

Fig. S2. Photosynthetic rates (mean ± SE, n = 6) of the coral *Acropora yongei* and the coralline alga *Sporolithon durum* exposed to the five seawater treatments. The colors represent the different treatments: Low DIC-High pH (dark green), Low DIC-Ambient pH (light green), Ambient (blue), High DIC-Low pH (orange), and High DIC – Ambient pH (red).

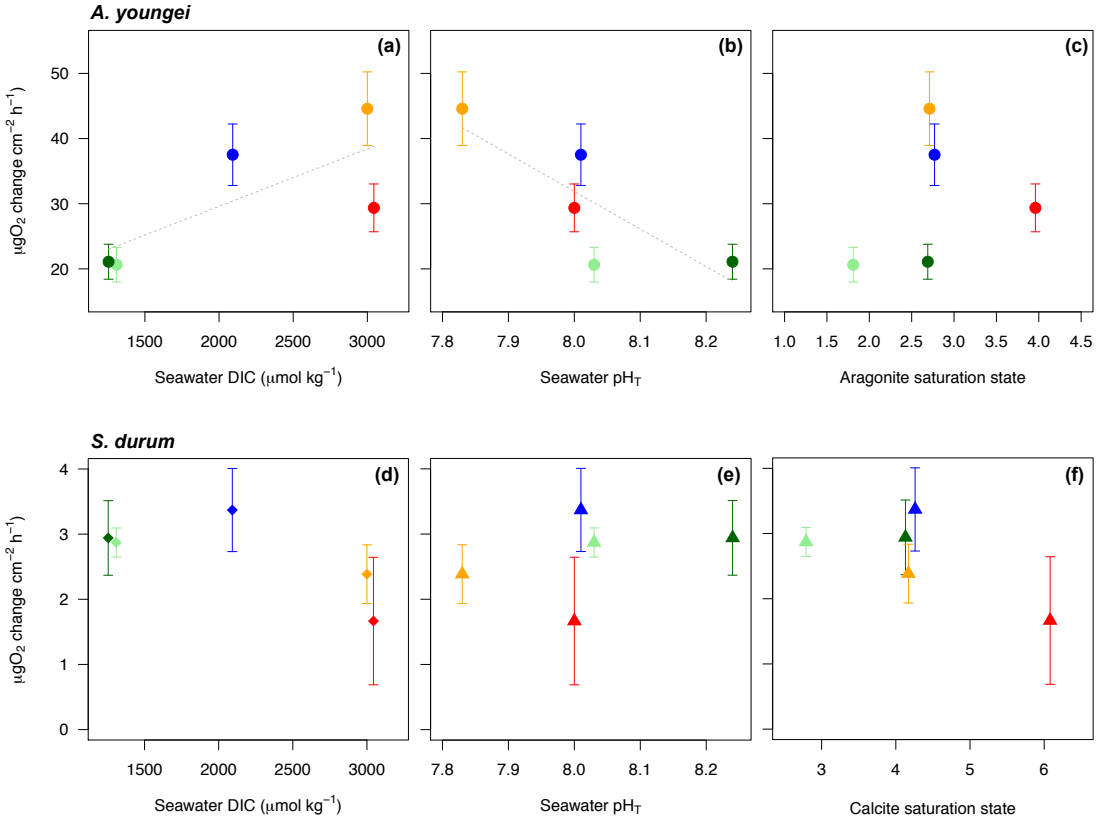

Fig. S3. Characteristic Raman spectra of coral and CCA analyzed in this study. The peaks in the region of ~700-720 cm^{-1} can be used to distinguish calcite and aragonite. Aragonite (blue) has a double peak < 710 cm^{-1} whereas high-Mg calcite (red) has a single broad peak > 710 cm^{-1}.